THE JOURNAL OF PHYSICAL CHEMISTRY B

pubs.acs.org/JPCB Article

Crowding-Induced Uncompetitive Inhibition of Lactate Dehydrogenase: Role of Entropic Pushing

Marin Matić,[‡] Suman Saurabh,[‡] Josef Hamacek,* and Francesco Piazza*

Cite This: https://dx.doi.org/10.1021/acs.jpcb.9b09596 Read Online

ACCESS | Metrics & More | Article Recommendations | Supporting Information

ABSTRACT: The cell is an extremely complex environment, notably highly crowded, segmented, and confining. Overall, there is overwhelming and ever-growing evidence that to understand how biochemical reactions proceed in vivo, one cannot separate the biochemical actors from their environment. Effects such as excluded volume, obstructed diffusion, weak nonspecific interactions, and fluctuations all team up to steer biochemical reactions often very far from what is observed in ideal conditions. In this paper, we use Ficoll PM70 and PEG 6000 to build an artificial crowded milieu of controlled composition and density in order to assess how such environments influence the biocatalytic activity of lactate dehydrogenase (LDH). Our measurements show that the normalized apparent affinity and maximum velocity decrease in the same fashion, a behavior reminiscent of uncompetitive inhibition, with PEG resulting in the largest reduction. In line with previous studies on other enzymes of the same family, and in agreement with the known role of a surface loop involved in enzyme isomerization and regulation of access to the active site, we suggest that the crowding matrix interferes with the conformational ensemble of the enzyme. This likely results in both impaired enzyme-complex isomerization and thwarted product release. Molecular dynamics simulations confirm that excluded-volume effects lead to an entropic force that effectively tends to push the loop closed, thereby effectively shifting the conformational ensemble of the enzyme in favor of a more stable complex isoform. Overall, our study substantiates the idea that most biochemical kinetics cannot be fully explained without including the subtle action of the environment where they take place naturally, in particular accounting for important factors such as excluded-volume effects and also weak nonspecific interactions when present, confinement, and fluctuations.

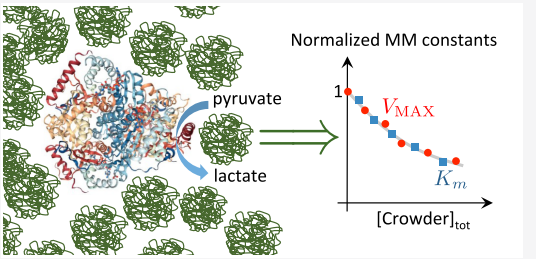

INTRODUCTION

The intracellular environment is a highly concentrated milieu of different macromolecules, whose combined concentration can exceed 400 g/L of macromolecules, representing up to 40% of the available cell volume.[1] In such an environment, the thermodynamic activity of a macromolecular solution changes with respect to the ideal diluted case.[2] This macromolecular crowding[3,4] reduces the free volume available for any other macromolecule present in the system (excluded-volume effect[5]), affecting its diffusion, equilibria, and reactivity. Since macromolecules cannot get closer to each other than the distance at which their surfaces meet, excluded-volume effects become more important for large molecules than for small ones.

Several aspects of macromolecular crowding are thoroughly investigated on proteins and particularly on enzymes by resorting to artificial crowding agents to recreate an environment that is no longer ideal but still far from the largely uncontrolled complexity of the cellular milieu. The most widely used model crowders are uncharged sugar-based polymers (Ficoll, dextran[6]) or poly(ethylene glycol) (PEG) based macromolecules. Ficoll is a sucrose polymer cross-linked with epichlorohydrin that forms pseudospherical particles, while PEGs and dextrans are linear flexible molecules.

In this context, there are many phenomena reported in the literature, such as stabilization of the native protein folds, protein−protein association, and increase in catalytic activity.[7] Some findings reveal opposite effects, that is, that macromolecular crowding promotes aggregation and destabilization of proteins and decreases enzymatic activity.[8] Although it is reasonable to speculate that purely excluded-volume effects might be generally little sensitive to the fine chemical details, soft intermolecular interactions, both among crowder molecules and between crowders and solute species, should also be considered to reconstruct the whole picture. During biochemical reactions, crowders primarily reduce the effective reaction volume, although soft interactions either with small molecules (substrates, products) or macromolecules such as other proteins may influence enzyme kinetics considerably.[9,10]

In this work, we concentrate on an enzymatic system of wide biochemical interest, that is, the transformation of pyruvate to lactate catalyzed by lactate dehydrogenase (LDH), a tetrameric

Received: October 11, 2019
Revised: December 23, 2019
Published: January 9, 2020

enzyme composed of catalytically independent subunits with a M_r around 35 kDa.[11] This reaction is well understood in diluted solutions and is also convenient for studies in crowded media, since small substrates and products do not significantly change the excluded volume. The enzymatic reaction can be experimentally followed via fluorescence spectroscopy as the decay of reduced nicotinamide adenine dinucleotide (NADH) fluorescence, probing indirectly the conversion of pyruvate to lactate. LDH catalyzes the direct transfer of a hydride ion from the reduced nicotinamide group of NADH to the C2 carbon of pyruvate,[12] but the rate-limiting step in this reaction is the closing of the mobile loop at the surface, which covers the substrate binding site.[13] Since there are two substrates, the kinetic mechanism of catalysis by LDH involves a ternary complex, which is of the compulsory-order type, with NADH binding to LDH first followed by pyruvate.[14−16] Our main purpose is to compare the reaction kinetics in the presence of different crowders that may significantly affect this complex catalytic reaction. The effect of dextran on this system has already been studied by Mas et al.,[17] who have reported a decrease of the enzyme maximum velocity, V_{MAX} with increasing crowding concentration, while the affinity, K_m, was found to be mostly insensitive to crowding. Those findings were interpreted globally as a signature of a mixed activation−diffusion control of this enzymatic reaction due to the crowding action of dextrans. More precisely, the authors of ref 17 argue that, in view of the comparable size between LDH and the crowders, the encounters between enzyme and substrate molecules are hindered, hence the reduction of the overall turnover rate k_{cat} and consequently of V_{MAX}. However, it may be argued that hindering enzyme−substrate encounters would reproduce the effect of obstructed diffusion of substrate molecules, that is, increasing the apparent affinity (K_m is inversely proportional to the enzyme−substrate diffusive encounter rate constant), which was not observed. Moreover, the effect of more globular crowding agents on the kinetics of LDH is still to be examined.

In this work, we investigate the effect of Ficoll PM70 and PEG 6000 on the LDH kinetics to understand their role in the catalysis of the transformation of pyruvate to lactate. The former crowding agents have approximately the same size as enzyme particles, while PEG 6000 allows us to investigate the so-called *protein regime* in crowding studies, that is, crowders smaller than diffusing proteins.[18] To account for the double substrate reaction, we vary the pyruvate concentration at a fixed concentration of NADH. Since the overall reaction follows a Michaelis−Menten mechanism, with apparent affinity and maximum velocity (as they depend on the fixed NADH concentration), we consider only initial rates of the reaction at different crowder concentrations and neglect product inhibition.[19] This also means that we can neglect the reverse enzyme−product recombination step (k_{-3}, eq 1), not, as often it is recounted, because the catalysis is irreversible but only because there simply is not enough product at the beginning of the reaction. Moreover, we selected a range of substrate concentrations for which overall the reaction exhibits no inhibition.[19−21] In addition, we applied a systematically specific protocol for a thorough homogenization of solutions containing substrate plus crowders before enzyme injection, in order to limit crowder aggregation.[22]

METHODS

Dynamic Light Scattering (DLS) of Crowder Solutions. Ten gram solutions of PEG 6000 or Ficoll PM70 at a mass fraction of 20% were prepared in ultrapure water. One part of the sample was left nonhomogenized, and the second was homogenized as described for the sake of comparison. The solutions were then filtered with syringe filters Millex GV 0.22 μm and sonicated for about 20 min in an ultrasonic bath with a frequency of 48 kHz (Bioblock Scientific, USA). DLS was performed on a Zetasizer Nano S at 25 °C with 300 s equilibration time. The measurements were performed with a 633 nm laser with backscatter detection geometry (175° angle). Three measurements were performed for each crowder for nonhomogenized and homogenized solutions and were averaged.

Preparation of Buffers and Solutions with Crowders. HEPES buffer (50 mM) with 1 mM EDTA was prepared by dissolving HEPES free acid (Sigma-Aldrich, USA) in "Milli-Q" ultrapure water (Merck, USA). pH was adjusted with NaOH to 7.43 ± 0.05 (21 °C) to be used at 7.3 ± 0.05 (30−32 °C) (HEPES buffer). Solutions of PEG 6000 (Merck, USA) and Ficoll PM70 (GE Healthcare, USA) were made in the HEPES buffer. Stock solutions (30 g) were made in a mass fraction ratio (% w/w) of 6.6%, 13.2%, 19.7%, 26.3%, 32.9%, and 39.5%. The solutions were stirred with a magnetic stirrer until all the crowders were dissolved. Each solution was then homogenized with a homogenizer 850 (Fisher Scientific, USA) using 7 mm × 115 mm dispersion element (11000 rpm, 7 cycles, each lasting 3 min with a 1 min break). Finally, the solutions were filtered either with syringe filters, Millex GV 0.22 μm with PVDF membrane (Merck, USA), or by vacuum filtration using 0.22 μm filters with nitrocellulose membrane (Merck, USA).

Preparation of Solutions for Kinetic Measurements. Stock solutions of 10 mM pyruvate and 5 mM NADH were prepared by dissolving sodium pyruvate (Sigma-Aldrich, USA) and Na_2NADH (Sigma-Aldrich, USA) in the HEPES buffer. Stock solutions of crowders were diluted in the HEPES buffer to the following w/w ratios: 5.3%, 10.5%, 15.8%, 21.1%, 26.3%, and 31.6%. The solutions were centrifuged for 1 min at 3000 rpm. Stock solutions of NADH and pyruvate were diluted to 1 mM and 2 mM, respectively, with the HEPES buffer, and stock solutions of crowders were diluted to desired concentrations. Final mass fractions used in kinetics measurements were 5%, 10%, 15%, 20%, 25%, and 30%. The preparation was accomplished by adding all the components made in corresponding diluted crowders (5.3% to 31.6%) into the microplate well and adding diluted enzyme without crowder. Solutions were kept on ice during preparation and stored in the refrigerator at +4 °C. NADH solutions were kept away from light and prepared and used only the same day. Pyruvate solutions were used up to 1 week after preparation. The solutions of crowders were stored at +4 °C.

Analysis of Kinetic Data. Initial velocities (v) were determined for each of the pyruvate concentrations and crowding conditions. Appropriate time ranges considered for linear regression were estimated with a Python script. The nonlinear fits of Michaelis−Menten plots (initial velocity versus pyruvate concentration) were performed in Qtiplot.[23] Best-fit values of the floating parameters, K_m and V_{MAX}, were acquired from the fit. Turnover numbers (k_{cat}) were calculated from the known enzyme concentrations as $k_{cat} = V_M/E_t$.

https://dx.doi.org/10.1021/acs.jpcb.9b09596
J. Phys. Chem. B XXXX, XXX, XXX−XXX

Molecular Dynamics Simulations. The structure of the human heart L-lactate dehydrogenase monomer was taken from the crystal structure with PDB id 1I0Z[24] by removing the coordinates of one of the monomers from the dimeric protein structure. The coordinates of the ligands (NADH and oxamate) were also removed. The structure was then coarse-grained using the shape-based coarse graining (SBCG) technique,[25] so that the 332 residues were represented by 110 effective beads. Harmonic bonds were created between the beads with a cutoff distance of 14 Å. The beads defining the loop region (shown in blue and green in Figure 4A,B) were assigned only 2 bonds each, those with their nearest neighbors along the loop. The total potential consisted of harmonic bond and angle bonded terms and a repulsive nonbonded vdW interaction (represented by a 12−6 Lennard-Jones potential) between the beads constituting the protein. The spring force constants were set at 20 kcal/(mol/Å^2) for all bonds. The angle coefficient was set to 6 kcal/(mol/rad^2) for the main body of the protein and 1 kcal/(mol/rad^2) for angle involving bead triplets in the loop.

The distance between a bead in the loop (shown in green) and another bead on the protein (gray) was used to define a closed and an open state. The gray bead is located on the periphery of the active site,[26] more precisely at the center of mass of the residues Glu236, Ala238, and Glu240. The loop bead is at the center of mass of Ser105, Lys106, and Leu107.

In order to mimic the presence of the substrate, which screens the repulsion between the arginines in the active site and the arginine residues on the loop, a mildly attractive Lennard-Jones interaction was introduced between the gray and green beads ($\varepsilon = 5k_BT$ and $\sigma = 6$ Å). This interaction (roughly one or two H-bonds worth) would weakly stabilize the closed state, thus mimicking the presence of the bound substrates, so that the effect of the crowders could be gauged by measuring the fluctuations about the closed state.

In order to measure the effect of crowding, another system was built that contained, in addition to the protein, spherical crowder beads of diameter 5 nm (shown in yellow) at two different volume fractions of 0.2 and 0.4. The crowder particles interacted among themselves and with the protein beads via a purely repulsive Weeks−Chandler−Andersen (i.e., 12−6 Lennard-Jones potential, cut off at its minimum and shifted up by the minimum depth). The simulations were performed with LAMMPS[27] with a time step of 3 fs. A Langevin thermostat was used to fix the temperature to 300 K with a relaxation parameter $\gamma = 25$ ps^{-1} to enforce overdamped dynamic.

RESULTS AND DISCUSSION

Homogenization of Crowded Solutions. Dynamic light scattering (DLS) measurements were carried out to evaluate the size distribution of the crowder molecules in solution before and after applying the homogenization protocol, the purpose of which was to remove aggregates that could alter the excluded volume in unwanted manners. The size distribution for a nonhomogenized Ficoll PM70 solution (20% w/w) by light intensity shows a bimodal distribution of particles: one major peak at 7 nm (close to the expected size) and the second around 100 nm in diameter, a telltale sign of the presence of aggregates. In contrast, there is only one peak for the mass distribution around 10 nm (Figure S1). Similar results were obtained for Ficoll PM70 solutions after homogenization (Figure S2). The size of Ficoll particles was characterized by two numbers (Table S1), namely, *z*-average and peak size. The polydispersity index (PDI) of Ficoll PM70 solutions is only slightly lowered after homogenization. The reported peaks correspond to 81.5% (nonhomogenized) and 83.2% of intensity distribution, meaning that the rest represents large peaks due to aggregation. However, the relative weight of the two peaks by mass indicates that there is a low quantity of aggregates in both cases (although they scatter a considerable part of the incoming light) and the monomeric particles dominate in number irrespective of the homogenization.

The effect of homogenization is more pronounced for PEG 6000. This can be seen for the distributions in Figure S3 and Figure S4. The size distributions by intensity display three peaks for the nonhomogenized solution, while the homogenized solution shows only one peak around 4 nm, as expected in the presence of monomers only. The two peaks at larger sizes flag the presence of aggregates or impurities that get fragmented after homogenization. Table S1 provides the calculated *z*-average for the nonhomogenized and homogenized solutions. The PDI is also substantially lowered for homogenized solution. In homogenized PEG solutions, the peak distribution around 4 nm accounts for 94.8% of the total intensity.

In summary, DLS enabled us to correctly estimate the size of particles through *z*-average values, except in the case of nonhomogenized solutions, where the peak size was more informative.[28,29] The homogenization protocol, combined with sonication, proved to be more effective in breaking apart aggregates in the case of PEG 6000, but it is expected to be also useful in the case of Ficoll PM70. The homogenization has been thus systematically applied to all samples of crowders prior to kinetic runs, in order to ensure reproducibility and afford reliable results.

Kinetics of Lactate Dehydrogenase. The Michaelis−Menten kinetics of LDH was investigated in the presence of Ficoll PM70 and PEG 6000 and can be described approximately as

$$\mathrm{E} + \mathrm{S} \underset{k_{-1}}{\overset{k_1}{\rightleftarrows}} \mathrm{ES} \underset{k_{-2}}{\overset{k_2}{\rightleftarrows}} \mathrm{EP} \underset{k_{-3}}{\overset{k_3}{\rightleftarrows}} \mathrm{E} + \mathrm{P} \tag{1}$$

In our case, S stands for pyruvate molecules, P is lactate, and E should be considered as the preformed NADH−LDH complex. Unfortunately, the initial velocity for high mass fractions (25% and 30%) could not be reasonably fitted and are not included in the following analysis. The data for Ficoll PM70 in Table S2 and Figure 1 show a decreasing trend of both the apparent K_m and V_{MAX} with the increase of the crowder concentration. This behavior results in a concomitant decrease of the turnover number k_{cat}. However, the ratio of the apparent K_m and V_{MAX}, which represents the specificity constant, also known as the enzyme *efficiency*, does not vary significantly with increasing mass fraction of crowders (Table S2), as K_m and V_{MAX} appear to decrease following the same law (Figure 3). It should be noticed that the error in the apparent affinity K_m increases with the mass fraction of Ficoll PM70. This can be attributed to a more difficult and less precise pipetting of more concentrated crowder solutions due to their increased viscosity.

For PEG 6000, we observed the same effect, namely, apparent K_m and V_{MAX} decreasing with increasing mass fraction of crowders (Table S3 and Figure 2). Similarly to what was found in the case of Ficoll, the ratio V_{MAX}/K_m stays constant no matter the mass fraction of PEG 6000 (Table S3). From

https://dx.doi.org/10.1021/acs.jpcb.9b09596
J. Phys. Chem. B XXXX, XXX, XXX−XXX

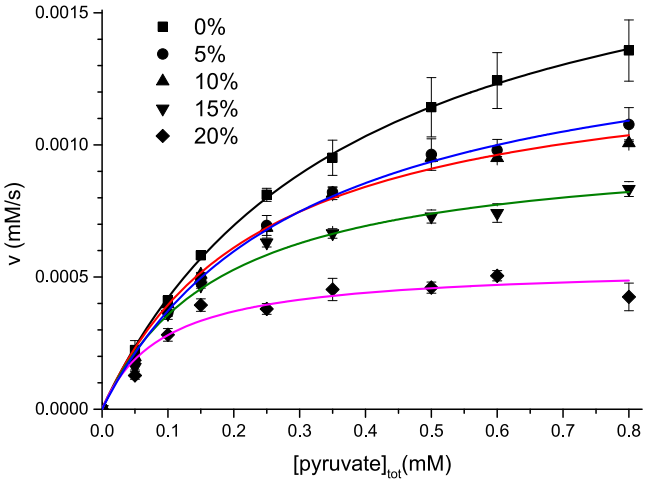

Figure 1. Nonlinear fits of Michaelis−Menten kinetics for lactate dehydrogenase in the presence of Ficoll PM70 from 0−20% w/w ($[pyruvate]_{tot}$ = 0.05−0.8 mM; $[NADH]_{tot}$ = 0.1 mM, $[E]_t$ = 7.33 nmol/L).

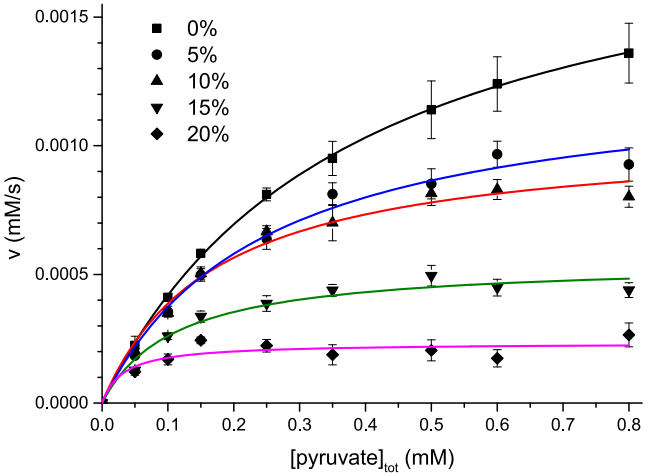

Figure 2. Nonlinear fit of Michaelis−Menten kinetics for lactate dehydrogenase in the presence of PEG 6000 from 0% to 20% w/w ($[pyruvate]_{tot}$ = 0.05−0.8 mM; $[NADH]_{tot}$ = 0.1 mM, $[E]_t$ = 7.33 nmol/L).

Table S3, it can be noticed that the error on the K_m again increases with the mass fraction of PEG 6000, but this effect is more pronounced in comparison to Ficoll PM70 (Table S2), reaching more than 50% of the apparent K_m value.

Overall, the apparent K_m and V_{MAX} values in the presence of both crowders were decreased considerably, up to 80−90% at 20% w/w (Figure 3), PEG reducing the affinity and maximum velocity more substantially than Ficoll.

Although the results are clear, interpreting our findings requires some care. First of all, we can rule out major contributions to the observed decrease in the MM constants coming from the altered molecular mobility of enzymes and substrate molecules in the presence of crowding. Although the increased viscosity and obstruction certainly slow down both enzyme and substrate diffusion, this appears not to interfere with the catalytic activity; otherwise we would have observed an *increased* apparent affinity, K_m, which is inversely proportional to the enzyme−substrate encounter rate and hence to the sum of their diffusion coefficients (an increase in diffusion *resistance*).[8] The same effect of crowders on the kinetic parameters was reported for two enzymes belonging to the same enzymatic class, alcohol dehydrogenase (ADH)[30] and malate dehydrogenase (MDH).[31] Interestingly, the magnitude of simultaneous reduction of maximum velocity and affinity for MDH was found to depend on the crowding agent, in agreement with our results, and reaction direction. Specifically, as in our case, it was the forward direction that displayed this behavior, the reverse direction exhibiting the opposite trend. It would be interesting to investigate whether the same observations would be made for LDH operating in the direction of lactate to pyruvate conversion. In both cases, the key observation proceeds from the relative magnitude of the catalytic rate, k_2 (i.e., conversion from ES to EP), and product release rate, k_3 (i.e., the forward step from EP to E + P). When $k_2 \gg k_3$, it can be shown that both affinity and maximum velocity are proportional to the product release rate, k_3.[31] Indeed, in the case of LDH, it is known that the rate of product release is in general slower than the rate of catalysis,[32,33] which corroborates the explanation that indeed crowding overall hinders product release.

This line of reasoning can be pushed farther by noting that the apparent K_m for this type of enzymes in the limit $k_2 \gg k_3$ is to a good extent described by the relation $K_m = k_3/k_1$, where k_1 is the rate of enzyme−substrate association guided by relative diffusion.[34] Taking into account that obstructed diffusion of small molecules is well described by a linear decrease of the kind[35]

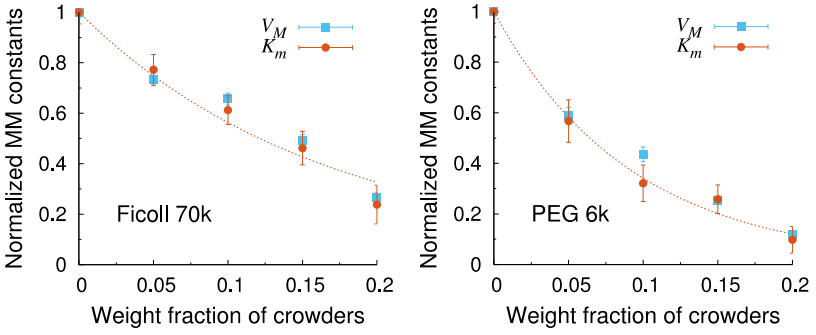

Figure 3. Relative change of the apparent Michaelis−Menten (MM) parameters K_m and V_{MAX} (±SEM) as a function of crowding level (w/w) for both crowding agents considered, Ficoll PM70 (left) and PEG 6000 (right). The dotted lines are one-parameter fits with eq 3 to the normalized affinity data.

https://dx.doi.org/10.1021/acs.jpcb.9b09596
J. Phys. Chem. B XXXX, XXX, XXX−XXX

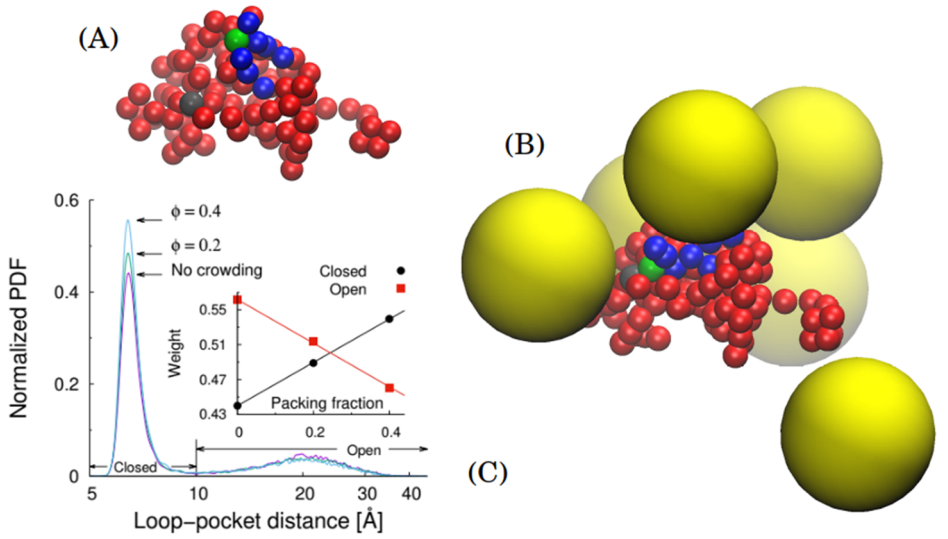

Figure 4. (A) Shape-based coarse grained model of the LDH monomer. The 332 amino acid protein has been represented by 110 effective beads. The loop is represented by blue (and a green) beads. In order to define the state of the loop (whether open or closed), we monitored the distance between the green (within the loop) and the gray (flanking the active site) beads. (B) Crowders are represented by inert hard spheres matching the size of Ficoll 70 monomers. (C) With no crowder in the vicinity, the loop is in a nearly balanced superposition of open and closed conformations (weights in the inset measure the areas under the two peaks). Upon increase of the crowding density, collisions with the protein push the loop more and more into the closed state, eventually reversing the relative weight in favor of the closed conformation (entropic pushing effect).

$$D(\varphi) = D_0\left(1 - \frac{3\varphi}{2}\right) \tag{2}$$

where φ is the crowding volume fraction and assuming that the slowing down of product release can be described by an Arrhenius-like rate to jump over an entropic barrier that increases with crowding concentration, we surmise that

$$K_m \propto \frac{k_3}{k_1} \propto \frac{e^{-\varphi/\varphi_0}}{1 - 3\varphi/2} \tag{3}$$

The existence of such an entropic barrier could be due, among other factors, to the crowding-induced reduction in the mobility of a surface loop that is known to regulate access to the active site in LDH.[26]

From the one-parameter fits reported in Figure 3, we get φ_0 = 0.09 for PEG 6000 and φ_0 = 0.14 for Ficoll 70. The agreement of this simple model with the experimental data is reasonably good, suggesting that indeed crowding-induced slowing down of product release is an important physical effect behind the observed phenomenology. It is instructive to remark that the simultaneous decrease of affinity and maximum velocity according to one and the same law in enzymology is the blueprint of uncompetitive inhibition. This is typically rationalized through the existence of an equilibrium between the complexes and corresponding *inactive* species, that is, isoforms where product release is strongly hampered. This is another way to picture the hindering action that crowders exert on product release, which is also corroborated by the results on other dehydrogenases, which share similar structure and mechanism of the product release with LDH.[36,37]

Alternatively, the decrease in apparent K_m could be explained via the stabilization of functional enzyme conformations, which would enhance the binding affinity of NADH. This could be a possibility for Ficoll PM70 as there are reports that its monomer, that is, sucrose, has a stabilizing effect on proteins.[38] However, it is not immediately clear why the same mechanism should be at work for PEG, which nonetheless exerts manifestly the same action on the forward kinetics of LDH. Different reports show that PEG has an influence on the conformation of proteins due to its hydrophobic nature increasing with the chain length and affects the hydration shell by removing layers of structured water from proteins.[8,39,40] Indeed, kinetic measurements of LDH activity in the presence of increasing concentrations of PEG 35000 (see Figure S5) showed that nearly all activity was lost at crowding concentrations as low as 5% w/w, hinting at the presence of interactions between such long PEG chains and the enzymes. However, it should be noticed that the influence of protein−crowder interactions on enzyme kinetics is not clear, as there are reports concluding in favor of both the increase and decrease of activity.[8,41]

Using Molecular Dynamics Simulations to Investigate Active Site Accessibility. It is well-known that in the ternary LDH complex a flexible loop closes over the two ligands, covering the active site and regulating its accessibility.[26] If our explanation of the experimental data holds true, that is, if crowding has an overall stabilizing effect on the complex, one would expect that structural fluctuations involving the loop should be altered by the presence of crowding, with the equilibrium between open and closed conformations displaced in favor of a larger weight of the latter ones. In order to explore this possibility in silico, we built a minimal molecular model of LDH to reconstruct the loop dynamics in the presence of crowding through molecular dynamics (MD) simulations (see Methods for the details of the model). The model and the main results are illustrated in Figure 4. As a relevant observable to monitor in time, we identified a reaction coordinate measuring the loop-active site distance (see Methods for more details). MD simulations on the order of 100 ns revealed that, in the absence of crowding, the loop fluctuates in a superposition of open and closed conformations, roughly 55% and 45%, respectively (see bimodal distributions in Figure 4C). It is also visible that fluctuations associated with the open conformations are much

https://dx.doi.org/10.1021/acs.jpcb.9b09596
J. Phys. Chem. B XXXX, XXX, XXX−XXX

broader (1−4.5 nm stretch) with respect to those characterizing the closed states (0.5−1 nm stretch). When the environment becomes crowded and excluded-volume effects become non-negligible, it can be clearly appreciated that the relative weights associated with open and closed conformations decrease and increase, respectively, until they swap, with the closed state becoming the most favored one beyond about 25% packing fraction (see inset in Figure 4C). This means that crowding is indeed expected to exert a stabilizing action on the complex. We might term the associated molecular mechanism crowding-induced *entropic pushing* of the loop. By favoring closed conformations through excluded-volume interactions between crowders and the loop beads, product release would be effectively hindered, in line with the interpretation of our experimental data on LDH kinetics.

CONCLUSIONS AND DISCUSSION

The forward (pyruvate to lactate) kinetics of LDH was investigated in the presence of two different globular crowding agents, namely, Ficoll PM70, a nearly spherical highly branched polysaccharide, and PEG 6000, a flexible random-coil polymer. In order to obtain reproducible results, it was important to sonicate and properly homogenize the samples with the crowders so as to efficiently get rid of spurious aggregates. Our results show unambiguously that the apparent affinity and maximum velocity at the chosen concentration of NADH decrease substantially with increasing crowding concentration, with PEG resulting in the most significant decrease. Remarkably, we find clear evidence that both crowding agents behave effectively as uncompetitive inhibitors, that is, the reduction of normalized affinity and maximum velocity are seen to collapse on the same curve. In agreement with previous studies, this strongly points to a general underlying mechanism for the parallel decrease of the Michaelis−Menten parameters. We suggest that the physical principle behind the observed phenomenology resides in the hindering action exerted by the crowding matrix on product release. Building on this idea, we surmise that a free-energy barrier that is mostly entropic and whose height increases linearly with crowding concentration has to be overcome. A simple Arrhenius hypothesis seems to substantiate our inference. Since we expect such free-energy barrier to be largely entropic, we predict that the observed reduction of normalized affinity and maximum velocity should not vary much with temperature. Measurements along these lines could substantiate our interpretation or, more generally, provide additional clues to pinpoint the physical origin of our experimental observations. Considerable insight into the molecular bases of the observed effective uncompetitive inhibition effect could be gained through molecular dynamics simulations. More precisely, we were able to spotlight an *entropic pushing* effect, whereby crowding leads to a reversal of the statistical weights of the open and closed conformations of the flexible loop that regulates access to the active site. In other words, excluded-volume effects lead to an entropic force that effectively pushes the loop closed, thereby stabilizing the complex and hampering product release. We observe that such entropic pushing effect should be a general phenomenon whenever access to active sites of proteins is regulated by flexible portions of the structure. Moreover, one also should expect that weak nonspecific interactions within the environment (macromolecular crowding agents, membranes, cytoskeletal elements, etc.) would further modulate this effect, thereby providing additional environmental control over biochemical reactions involving binding and release.

It is interesting to recall that the same effect reported in this paper (i.e., simultaneous decrease of both kinetic parameters) was also observed in the presence of increasing concentrations of small viscogenic molecules (glycerol, sucrose). In particular, the Demchenko and co-workers[42] concluded that the conformational motion leading to the ternary complex conformation, involving a large rearrangement of the loop, is rate-limiting for both directions of the reaction catalyzed by LDH. Therefore, in the presence of small viscogenous agents, the increased microviscosity alters the loop dynamics, hindering enzyme isomerization and leading to a stabilization of nonproficient complex conformations. It should be observed however that, in general, the effect on enzyme kinetics of small viscogenous molecules and large polymeric cosolvents (such as PEG and Ficoll) could be very different. The notion of viscosity becomes a rather subtle one, as microscopic and macroscopic viscosities could differ substantially and in a way that is still not entirely clear from the microscopic point of view.[43] Taken together, these considerations suggest that *any* interference with the loop dynamics is likely to meddle with enzyme isomerization and lead to a population shift in the complex, resulting in the same effect on the measured kinetic parameters. More generally, it is likely that both the chemical step and product release are slaved to the isomerization step involving fluctuations of the loop at the active site entrance, which means that the microscopic origin of the apparent inhibition most likely involves both impaired isomerization and hampered product release.

Although MD simulations suggest that entropic pushing alone could be enough to cause the observed uncompetitive inhibition effect, it should be observed that the concurrent action of weak binding of the crowders to the enzyme could not be ruled out in principle, although it is not clear in what direction that would affect the kinetics. There is some experimental evidence that long PEG polymers indeed may display weak interactions with small proteins,[44] challenging the commonly accepted wisdom that PEG polymers are essentially inert crowders.[7] It is not clear how PEG would interact with larger complexes such as LDH. Moreover, we found that Ficoll 70, which is to the best of our knowledge still considered a rather inert crowder, causes the same exact effect as PEG, suggesting that excluded-volume effect is key to rationalize the observed changes in enzyme kinetics. Interestingly, it has been reported that zwitterionic poly(sulfobetaine methacrylate) (pSBMA) polymers are more inert than PEG.[44] Therefore, it would be informative to perform kinetics measurements with pSBMA polymers of the same size and compare with PEG. In principle, this could help tell entropic from enthalpic effects on enzyme kinetics.

In summary, we believe that our study contributes to reinforce the general idea that biochemical kinetics cannot be fully apprehended without accounting for the often-elusive action of the environment where they take place naturally. More generally, we observe that this not only entails investigating excluded-volume effects but might also include importantly the subtle effects of weak nonspecific interactions, confinement, and fluctuations, which can team in crafty ways to steer the reactions toward regimes that are very far from the simplistic picture of a dilute solution in a test tube.

https://dx.doi.org/10.1021/acs.jpcb.9b09596
J. Phys. Chem. B XXXX, XXX, XXX−XXX

■ ASSOCIATED CONTENT

Supporting Information

The Supporting Information is available free of charge at https://pubs.acs.org/doi/10.1021/acs.jpcb.9b09596.

Experimental details for kinetic measurements, DLS data, kinetic parameters, size distribution of particles for Ficoll 70 and PEG 6000 solutions, and kinetic measurements of LDH activity in the presence of 5% (w/w) PEG 35000 crowders (PDF)

■ AUTHOR INFORMATION

Corresponding Authors

Josef Hamacek − *Centre de Biophysique Moléculaire (CBM), CNRS UPR 4301, Université d'Orléans 45071 Orléans, France*; Email: josef.hamacek@cnrs.fr

Francesco Piazza − *Centre de Biophysique Moléculaire (CBM), CNRS UPR 4301, Université d'Orléans 45071 Orléans, France*; orcid.org/0000-0003-0205-3790; Email: francesco.piazza@cnrs-orleans.fr

Authors

Marin Matić − *Centre de Biophysique Moléculaire (CBM), CNRS UPR 4301, Université d'Orléans 45071 Orléans, France*

Suman Saurabh − *Centre de Biophysique Moléculaire (CBM), CNRS UPR 4301, Université d'Orléans 45071 Orléans, France*

Complete contact information is available at: https://pubs.acs.org/10.1021/acs.jpcb.9b09596

Author Contributions

‡M.M. and S.S. contributed equally. M.M. performed the experiments. S.S. performed molecular dynamics simulations. M.M., J.H., and F.P. analyzed the data and wrote the paper.

Notes

The authors declare no competing financial interest.

■ ACKNOWLEDGMENTS

This study was supported by the CNRS Orléans (Center for Molecular Biophysics) and the ARD 2020 Cosmetosciences.

■ ABBREVIATIONS

LDH, lactate dehydrogenase; PEG, poly(ethylene glycol); NADH, nicotinamide adenine dinucleotide

■ REFERENCES

(1) Ellis, R. J. Macromolecular crowding: Obvious but underappreciated. *Trends Biochem. Sci.* **2001**, *26*, 597−604.

(2) Minton, A. P. The Influence of Macromolecular Crowding and Macromolecular Confinement on Biochemical Reactions in Physiological Media. *J. Biol. Chem.* **2001**, *276*, 10577−10580.

(3) Rosen, J.; Kim, Y. C.; Mittal, J. Modest protein-crowder attractive interactions can counteract enhancement of protein association by intermolecular excluded volume interactions. *J. Phys. Chem. B* **2011**, *115*, 2683−2689.

(4) Sarkar, M.; Li, C.; Pielak, G. J. Soft interactions and crowding. *Biophys. Rev.* **2013**, *5*, 187−194.

(5) Minton, A. P. Excluded volume as a determinant of macromolecular structure and reactivity. *Biopolymers* **1981**, *20*, 2093−2120.

(6) Batra, J.; Xu, K.; Qin, S.; Zhou, H. X. Effect of macromolecular crowding on protein binding stability: Modest stabilization and significant biological consequences. *Biophys. J.* **2009**, *97*, 906−911.

(7) Kuznetsova, I. M.; Turoverov, K. K.; Uversky, V. N. What macromolecular crowding can do to a protein. *Int. J. Mol. Sci.* **2014**, *15*, 23090−23140.

(8) Mittal, S.; Chowhan, R. K.; Singh, L. R. Macromolecular crowding: Macromolecules friend or foe. *Biochim. Biophys. Acta, Gen. Subj.* **2015**, *1850*, 1822−1831.

(9) Mukherjee, S. K.; Gautam, S.; Biswas, S.; Kundu, J.; Chowdhury, P. K. Do Macromolecular Crowding Agents Exert Only an Excluded Volume Effect? A Protein Solvation Study. *J. Phys. Chem. B* **2015**, *119*, 14145−14156.

(10) Aumiller, W. M.; Davis, B. W.; Hatzakis, E.; Keating, C. D. Interactions of macromolecular crowding agents and cosolutes with small-molecule substrates: Effect on horseradish peroxidase activity with two different substrates. *J. Phys. Chem. B* **2014**, *118* (36), 10624−10632.

(11) Markert, C. L. Lactate dehydrogenase. Biochemistry and function of lactate dehydrogenase. *Cell Biochem. Funct.* **1984**, *2*, 131−134.

(12) McClendon, S.; Zhadin, N.; Callender, R. The approach to the Michaelis complex in lactate dehydrogenase: The substrate binding pathway. *Biophys. J.* **2005**, *89*, 2024−2032.

(13) Pineda, J. R. E. T.; Callender, R.; Schwartz, S. D. Ligand Binding and Protein Dynamics in Lactate Dehydrogenase. *Biophys. J.* **2007**, *93*, 1474−1483.

(14) Zewe, V.; Fromm, H. J. Kinetic studies of rabbit muscle lactate dehydrogenase. *J. Biol. Chem.* **1962**, *237*, 1668−1675.

(15) Cleland, W. The kinetics of enzyme-catalyzed reactions with two or more substrates or products. *Biochim. Biophys. Acta, Spec. Sect. Enzymol. Subj.* **1963**, *67*, 188−196.

(16) Cornish-Bowden, A. Reactions of More than One Substrate. *Fundamentals of enzyme kinetics*, 4th revised ed.; Wiley-Blackwell: Weinheim, Germany, 2012; pp 189−227.

(17) Balcells, C.; Pastor, I.; Vilaseca, E.; Madurga, S.; Cascante, M.; Mas, F. Macromolecular Crowding Effect upon in Vitro Enzyme Kinetics: Mixed Activation−Diffusion Control of the Oxidation of NADH by Pyruvate Catalyzed by Lactate Dehydrogenase. *J. Phys. Chem. B* **2014**, *118*, 4062−4068.

(18) Palit, S.; He, L.; Hamilton, W. A.; Yethiraj, A.; Yethiraj, A. Combining Diffusion NMR and Small-Angle Neutron Scattering Enables Precise Measurements of Polymer Chain Compression in a Crowded Environment. *Phys. Rev. Lett.* **2017**, *118* (9), 097801.

(19) Coulson, C. J.; Rabin, B. R. Inhibition of lactate dehydrogenase by high concentrations of pyruvate: The nature and removal of the inhibitor. *FEBS Lett.* **1969**, *3*, 333−337.

(20) Gutfreund, H.; Cantwell, R.; McMurray, C. H.; Criddle, R. S.; Hathaway, G. The kinetics of the reversible inhibition of heart lactate dehydrogenase through the formation of the enzyme-oxidized nicotinamide-adenine dinucleotide-pyruvate compounds. *Biochem. J.* **1968**, *106*, 683−7.

(21) Eggert, M. W.; Byrne, M. E.; Chambers, R. P. Impact of High Pyruvate Concentration on Kinetics of Rabbit Muscle Lactate Dehydrogenase. *Appl. Biochem. Biotechnol.* **2011**, *165*, 676.

(22) Grossutti, M.; Dutcher, J. R. Correlation Between Chain Architecture and Hydration Water Structure in Polysaccharides. *Biomacromolecules* **2016**, *17* (3), 1198−1204.

(23) Vasilief, I. QtiPlot. https://www.qtiplot.com/, 2019.

(24) Read, J. A.; Winter, V. J.; Eszes, C. M.; Sessions, R. B.; Brady, R. L. Structural basis for altered activity of M- and H-isozyme forms of human lactate dehydrogenase. *Proteins: Struct., Funct., Genet.* **2001**, *43*, 175−185.

(25) Freddolino, P. L.; Arkhipov, A.; Shih, A. Y.; Yin, Y.; Chen, Z.; Schulten, K. Application of Residue-Based and Shape-Based Coarse Graining to Biomolecular Simulations. In *Multiscale Simulation Methods in Molecular Sciences*; Grotendorst, J., Attig, N., Blügel, S., Marx, D., Eds.; Forschungszentrum Jülich, 2009; Vol. *42*, pp 445−466.

(26) Gerstein, M.; Chothia, C. Analysis of protein loop closure. Two types of hinges produce one motion in lactate dehydrogenase. *J. Mol. Biol.* **1991**, *220* (1), 133−149.

(27) Plimpton, S. Fast Parallel Algorithms for Short-Range Molecular Dynamics. *J. Comput. Phys.* **1995**, *117*, 1−19.
(28) GE Healthcare. Ficoll PM70, Ficoll PM400. 2007, https://www.gelifesciences.co.jp/catalog/pdf/18115827.pdf.
(29) Armstrong, J. K.; Wenby, R. B.; Meiselman, H. J.; Fisher, T. C. The hydrodynamic radii of macromolecules and their effect on red blood cell aggregation. *Biophys. J.* **2004**, *87*, 4259−4270.
(30) Wilcox, A. E.; LoConte, M. A.; Slade, K. M. Effects of macromolecular crowding on alcohol dehydrogenase activity are substrate-dependent. *Biochemistry* **2016**, *55*, 3550−3558.
(31) Poggi, C. G.; Slade, K. M. Macromolecular crowding and the steady-state kinetics of malate dehydrogenase. *Biochemistry* **2015**, *54*, 260−267.
(32) Whitaker, J. R.; Yates, D. W.; Bennett, N. G.; Holbrook, J. J.; Gutfreund, H. The identification of intermediates in the reaction of pig heart lactate dehydrogenase with its substrates. *Biochem. J.* **1974**, *139*, 677−97.
(33) Stinson, B. R. A.; Gutfreund, H. Transient-Kinetic Studies of Pig Muscle Lactate Dehydrogenase. *Biochem. J.* **1971**, *121*, 235−240.
(34) Northrop, D. B. On the Meaning of Km and V/K in Enzyme Kinetics. *J. Chem. Educ.* **1998**, *75*, 1153.
(35) Jonsson, B.; Wennersrom, H.; Nilsson, P. G.; Linse, P. Self-diffusion of small molecules in colloidal systems. *Colloid Polym. Sci.* **1986**, *264* (1), 77−88.
(36) Leskovac, V.; Trivić, S.; Peričin, D. The three zinc-containing alcohol dehydrogenases from baker's yeast, Saccharomyces cerevisiae. *FEMS Yeast Res.* **2002**, *2*, 481−494.
(37) Goward, C. R.; Nicholls, D. J. Malate dehydrogenase: A model for structure, evolution, and catalysis. *Protein Sci.* **1994**, *3*, 1883−1888.
(38) Arakawa, T.; Timasheff, S. N. The stabilization of proteins by osmolytes. *Biophys. J.* **1985**, *47*, 411−414.
(39) Tubio, G.; Nerli, B.; Picó, G. Relationship between the protein surface hydrophobicity and its partitioning behaviour in aqueous two-phase systems of polyethyleneglycol - dextran. *J. Chromatogr. B: Anal. Technol. Biomed. Life Sci.* **2004**, *799*, 293−301.
(40) Wu, J.; Zhao, C.; Lin, W.; Hu, R.; Wang, Q.; Chen, H.; Zheng, J.; et al. Binding characteristics between polyethylene glycol (PEG) and proteins in aqueous solution. *J. Mater. Chem. B* **2014**, *2* (20), 2983−2992.
(41) Totani, K.; Ihara, Y.; Matsuo, I.; Ito, Y. Effects of macromolecular crowding on glycoprotein processing enzymes. *J. Am. Chem. Soc.* **2008**, *130*, 2101−2107.
(42) Demchenko, A. P.; Rusyn, O. I.; Saburova, E. A. Kinetics of the lactate dehydrogenase reaction in high-viscosity media. *Biochim. Biophys. Acta, Protein Struct. Mol. Enzymol.* **1989**, *998* (2), 196−203.
(43) Szymański, J.; Patkowski, A.; Wilk, A.; Garstecki, P.; Holyst, R. Diffusion and viscosity in a crowded environment: From nano- to macroscale. *J. Phys. Chem. B* **2006**, *110* (51), 25593−25597.
(44) Wu, J.; Zhao, C.; Hu, R.; Lin, W.; Wang, Q.; Zhao, J.; Zheng, J.; et al. Probing the weak interaction of proteins with neutral and zwitterionic antifouling polymers. *Acta Biomater.* **2014**, *10* (2), 751−760.

https://dx.doi.org/10.1021/acs.jpcb.9b09596
J. Phys. Chem. B XXXX, XXX, XXX−XXX